ACTA IMEKO
ISSN: 2221-870X
September 2024, Volume 13, Number 3, 1 - 11

Thrust ball bearing fault identification from visualized data using optimized deep network

S. Mary Evanchalin[1], T. Milton[2], F. M. Tamil Selvi[3], Anagha Chaudhari[4], Ashish Mogra[5]

[1] *Nandha Engineering College, Erode, Tamil Nadu 638052, India*
[2] *Paavai Engineering College, Namakkal, Tamil Nadu 637018, India*
[3] *Bethlehem Institute of Engineering, Ulaganvillai, Tamil Nadu 629157, India*
[4] *Assistant Professor, Department of Computer Engineering, Pimpri Chinchwad College of Engineering, Pune, India*
[5] *Department of Mechanical Engineering, School of Technology Management & Engineering, SVKM's Narsee Monjee Institute of Management Studies (NMIMS), Deemed-to-University, Chandigarh-160014, India*

ABSTRACT
Bearings are the most common components employed in machine parts. The bearings' movement facilitates the smooth motion. They also help with friction reduction. The faults in bearings are often caused by tribological parameters. Various methods have been developed to identify faults in bearings, but they often fail to predict these accurately. This work has concentrated on designing an effective fault-recognizing model. Therefore, a framework, the Zebra-based Radial Basis Prediction Mechanism (ZbRBPM), was proposed in this work. Initially, the bearing datasets are collected, and mineral oil (MO) lubrication is added to minimize wear and friction. The primary goal of the work is to detect and classify the fault in the thrust ball bearing. The bearing vibration data included a normal vibration signal, a ball fault, and inner and outer race faults. Hence, Zebra fitness is enhanced for the optimization of tribological parameters and fault identification. The proposed model is executed in the MATLAB system. Finally, performance criteria like accuracy, precision, recall, F-score, error rate, computation time, speed, specific wear rate, friction torque, and energy consumption are validated. The performance of the proposed ZbRBPM gains better accuracy rate as 99.5 %, 99 % of precision and f-score and 99.4 % of recall. Also it significantly reduced the prediction error rate into 0.5 % with lower computation time and very low wear and friction.

Section: RESEARCH PAPER

Keywords: fault identification; wear and friction; bearings; lubrication

Citation: S. M. Evanchalin, T. Milton, F. M. Tamil Selvi, A. Chaudhari, A. Mogra, Thrust ball bearing fault identification from visualized data using optimized deep network, Acta IMEKO, vol. 13 (2024) no. 3, pp. 1-11. DOI: 10.21014/actaimeko.v13i3.1839

Section Editor: Laura Fabbiano, Politecnico di Bari, Italy

Received March 5, 2024; **In final form** July 24, 2024; **Published** September 2024

Corresponding author: S. Mary Evanchalin, e-mail: evanchalinece@gmail.com

1. INTRODUCTION

In Mechanical systems, the application of bearings performs a crucial role in developing the efficiency of mechanical systems completely and minimizing frictional losses [1]. With the improvement in the machining and materials bearing, the authenticity of the bearings is progressively established. Performing bearings in the machinery of wind power and mining in frigid environments are exposed to the threat of particle contaminants, resulting in the devastating defeat of the rolling bearings [2]. Rolling element bearings are an integral portion of the rotating machines. Machine performance may fail if the fault of bearings is not properly detected. It is very necessary to detect the bearing fault for the continuous functioning of the machine [3]. In rolling components, tear and wear harm the joining zone of the rolling elements with ease. In the present day, bearings are one of the admirable innovations that perform a crucial function in the wear reduction of all rotating components. Bearings are categorized into three types: roller bearings, ball bearings, and bushed bearings. Of these, based on performance and durability, ball bearings were frequently used [4]. Ball bearings are composed of three components, i.e., balls, an inner ring, and an outer ring. Their rotational friction is less and produces minimum heat when compared to the other bearings. The good-condition bearings will maintain the rotating parts in a significant pattern with one another and impede the development of abnormalities. The performance and results of the machine are affected by the faulty bearing [5]. Particle breakage results from the friction pair's slow formation of a shear zone that is inclined to the left as the granular materials become compressed and

sheared. The particle breaking causes the friction coefficient to rise and the load-bearing capacity to decrease [6]. The inner film's dynamic coefficients and static performance parameters are significantly impacted by the clearance ratio, while the outside film is unaffected. On the other hand, both the inner and outer films are affected by the vertical load [7]. Tribology is the science of friction, lubrication, and wear. It plays a critical role in understanding and optimizing the performance of thrust ball bearings. Bearing dynamics deal with the forces, motions, and vibrations experienced by the bearing. Some studies have concentrated on the tribology's intersection action and bearing dynamics [8]. The rotor system in the rolling bearing is broadly exploited in rotating mechanical equipment [9]. Their performance impacts the maintenance period of the entire machine. Hence, the study of bearing lubrication action and the dynamic execution of rotors assisted by bearing.

Elastohydrodynamic Lubrication (EHL) film denseness formulation is used to attain a graphing solution to evaluate the quality of lubrication. The elastohydrodynamic lubrication establishment appears in the rolling bearings providing rise to small contact of arbitrary shapes between the raceway and ball [10]. The rolling bearings are utilized in so many different types of devices; therefore it is imperative that any issues are found as soon as possible. While vibration analysis is frequently employed in rolling bearing diagnosis, an acoustic emission (AE) procedure mentioned in [11] may be able to identify the breakdown of these bearings early. The electrical ball bearing damage evolution can also be measured using surface characteristics as a quantitative damage scale [12]. In the last decade of years, machine learning algorithms have been described as the efficient method for identifying the robustness and the fault of the machine equipment [13].

In order to analyse and identify the various fault severities of the outer race bearing fault in an induction motor, machine learning, and artificial intelligence are used. Because it retains the most discriminative and useful information, which leads to a high-performance condition characterization, linear discriminant analysis is significant. Additionally, a classifier based on neural networks enables the validation of the efficacy of fusion data from various physical magnitudes to address the diagnosis of several fault severities that manifest in the outer race of the bearing [14]. Related algorithms are frequently employed in the diagnosis and identification of rotor problems in conjunction with other signal-processing techniques. A novel multi-source vibration signal fusion technique is presented to address the issue of a single sensor's vibration signal being too solitary [15]. The majority and broad use of the commercial methodology for detecting a fault, estimating acoustic, and analysing vibration signals. Here, the fault detection is based on combining the Hilbert transmute, autocorrelation, and the wavelet packet. For estimating acoustic sound pressure, sound intensity, and the acoustic emission method are used. Analysing vibration signals is acquired by the shock pulse method, frequency, and vibration in time. [16] In the event of an equal weight distribution, the load, interaction stress, and interface deformation of this ball exceed those of all the other balls. It restricts a practical bearing's ability to support loads in relation to its theoretical static load rating [17] Two types of precursor were found, which most likely caused pitting or spalling during the subsequent rolling contact. One is the surface imperfections, like heavy machining marks, scratches, and slag holes, on the rolling ball or the raceway. The other is a machining-induced Nano-crystalline layer in the outermost layer surrounding the raceway's surface [18]. Also determines that a common high-speed thrust angular associate ball bearing is sorted. The assembled facet standard of rolling components and the raceway were characterized. Bearings use lubrication to reduce friction and wear between moving parts. Insufficient lubrication and elevated operational issues could increase friction, overheating, and wear [19]. It leads to surface damage such as scoring, corrosion, and galling. Fault identification in rolling bearings is critical for avoiding catastrophic failures, decreasing downtime, lowering repair costs, and maintaining machinery integrity and safety. Considering these demerits, the rolling bearing is considered for this study. The key contributions of this work are described as follows,

- Initially, The thrust ball bearing dataset is trained in the MATLAB system
- Then a novel ZbRBPM was introduced with the needed prediction features for predicting the fault.
- Accordingly, the thrust ball bearings' actions like wear and friction were evaluated and gathered.
- To achieve the finest optimal result, features like MO are added and the wear and friction are computed one more time.
- Moreover, to obtain the best tribological criteria, the zebra fitness is adjoined to the radial basis Prediction mechanism classification.
- The tribological criteria attached to the fitness activity are tuned up to the most feasible range.
- Finally, the performance criteria such as Accuracy, precision, Recall and F score, wear, and friction were calculated and compared with other models.

This research paper includes the related work in section two, the system model in section three, the proposed method in section four, the performance validation for the proposed model determined in section five, and the work conclusion in section six.

2. RELATED WORK

A few recent associated works are described as follows;

Wu et al. [19] described to development of the essentials of rolling bearings and three texture types were improved on the surface leading to the thrust ball bearing. Three textures developed namely gradient groove texture, groove texture, and dimple. The results of the vibration of gradient groove textured and non-textured bearings are made a comparison among them and it outcomes decrease by 49.1 % and 24.6 % respectively. The frequency analysis results showed that the textures concealed the intermediate the inflated frequency decreased by 65.3 % and the friction torque was reduced by 10.5 %.

Bhardwaj et al. [20] have implemented the tribodynamic accomplishment manners of the thrust ball bearing engaging micro-grooves in the static uppermost ring. It is determined by utilizing grease and oil lubricants. The operation takes place in light loads and the speed range varies from 1.8 to 4.0 m/s. The consequences of the microgroove static races are a rise in temperature, bearing vibrations, and frictional torque. The bulk rise in temperature of 14-26 %, bearing vibrations of 7-34 %, and frictional torque of 14-21 % were obtained from the microgroove. As a result, the microgroove oil lubricated in tribodynamic gets significant development when made a comparison to the grease lubricated of functioning specification.

Lu-Minh et al. [21] describe the execution estimation by utilizing a fretting tribometer for the mechanical transmission of

three greases. In the standard ASTM D4170, the thrust ball bearings were determined to evaluate the load diffusion relying on the upper or lower or angular position. Later 5 h solely, 30 Hz of frequency at room temperature and 2450 N of load is reported. The lower position thrust ball bearing is worn more than the top position. The mass loss with the grease obtained in the lowest position was utilized in food industries.

Shan et al. [22] demonstrate inside the ball bearing the oil air multistep flow attributes are exposed by contract for difference and ball bearing analysis of the lubrication model. Here, the ball bearing is developed by the complex bearing of boundary shape. The model is separated into mesh density and the hexahedron elements close to the connection zone increase, elevating the accuracy and the convergence. The outcome describes the appropriate size of clearance and it improves the internal flow and the ball bearing performance. Moreover, the Voltage-Induced Damage Progression of Thrust ball bearing [23], and Self-Lubricating Polytetrafluoroethylene cages and Surface-textured raceways (SLPS) [24] are the recent methodologies that attains good bearing resistance [25], regarding wear [26], friction torque [27] and energy consumption in bearing application [28].

For fault identification and visualization, Mahesh et al. [29] discussed the 1D Convolutional Networks and t-distributed Stochastic Neighbour Embedding (t-SNE) outperform conventional signal processing techniques and machine learning models. They can improve fault detection performance in noisy environments by extracting features from raw sensor data, learning features at several levels, differentiating between fault types and severity levels, and modelling nonlinear data connections. Because they are scalable, resilient to noise, and flexible enough to adjust to complicated fault patterns, their complexity usually makes them harder to understand.

Pham et al. [30] described a generalized adversarial neural technique that uses AE monitoring signals in a 2-D spectrogram to diagnose bearing faults. In contrast to low-sample, unbalanced, and noisy datasets, the architectures and training strategy enhance convolution network-based classifier performance. On ten trial datasets, the approach performs better than Decision-based generalized networks and other deep learning techniques. The enhanced technique is a viable strategy for intelligent factories in actual working contexts since it achieves great precision and quick convergence. However, generalized network-based techniques can be a resource and computationally intensive, especially while they're being trained.

Nemani et al. [31] presented a feature weighting technique based on principles of physics to mitigate the degradation of the model due to variations in data distribution. It predicts bearing health class by using vibration signals to create an envelope order spectrum. The controller-based convolutional network model, which consists of Convolutional networks plus a feature weighting layer, gives discriminative fault features larger weights and is resistant to speed variations. The approach is versatile and simple to use with a variety of models. However, in these realistic industrial contexts, this approach performs ineffective and erroneous diagnoses.

In order to detect problems, Xingchen et al. [32] suggested a novel Modified tuned convolutional network model that analyses three-axis vibration data from an accelerometer inside rollers. After training on radial vibration data using dual-channel Decision networks, the model has demonstrated no misclassification between problematic and normal bearings. At a noise ratio of less than 10 dB, it attains accuracy levels of 95.44 %, 95.52 %, and 90.08 %. Additionally, the model outperforms three-channel Decision-based convolutional networks in terms of accuracy, achieving values that are 26.06 %, 11.23 %, and 17.12 % higher. Nevertheless, this approach does not prioritize robustness and transferability to the TBM engineering site.

In addition, the demerits of the discussed literature are insufficient feature selection and predictive behaviour that reduce the prediction accuracy. Also, the vibration signal of the bearing is more noisy and is not readable by the traditional neural network principles. Also, the speed of the fault prediction system is too low with a high error rate due to insufficient features. So, the optimized deep network is considered for this study.

The key objective of this study is to find the faulty signal from the thrust ball bearing using the vibration image data. Second, the tribological behaviour was optimized to the desired level. These two problems were mainly solved using the Zebra fitness solution.

3. SYSTEM MODEL WITH PROBLEM

Thrust ball bearing plays an essential role in modern technology. In this, it is essential to find out the faults in the thrust ball bearing. Identifying and maintaining the component's fault is very important to accelerate the functioning efficiency. In the past, the prediction mechanism based on mathematical and optimization models was implemented for predicting the bearing faults, but a suitable outcome was not attained. The issues that were recorded by the traditional prediction model are described in Figure 1. In addition, a few step processes such as pre-processing, feature extraction, and prediction were executed for detecting the fault signal. If the above-suggested process is not done properly by the traditional models due to feature limitations, that has reported wrong prediction.

Hence, this present proposed research has designed a novel optimized deep network for identifying faults from the visualized data.

4. PROPOSED METHODOLOGY

A novel Zebra-based Radial Basis Prediction Mechanism (ZbRBPM) was introduced in this study to recognize the fault from the visualized data and tune the parameters. The proposed model ZbRBPM is optimized to enhance tribology criteria like wear and friction. Further Mineral oil (MO) was added to develop the bearings functions. The vibration signal has been observed on the designed model. The performance validation for wear and friction is noted. Finally, the fault is identified based on

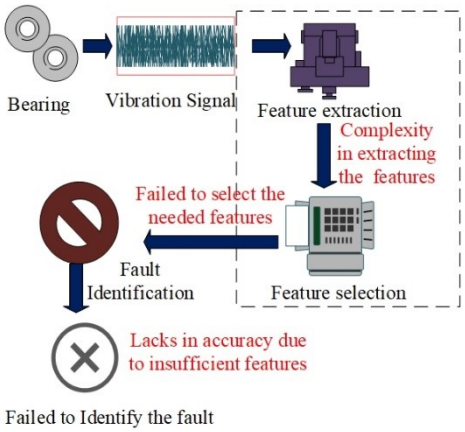

Figure 1. Fault identification with issues.

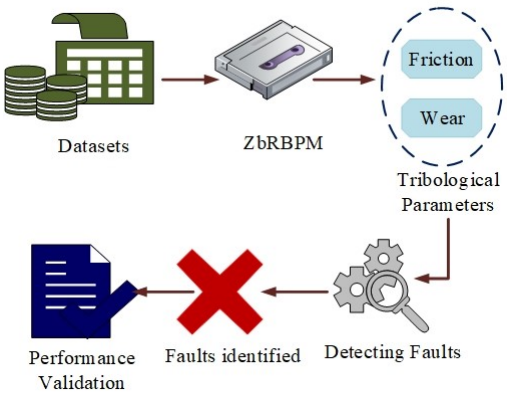

Figure 2. CAPTION.

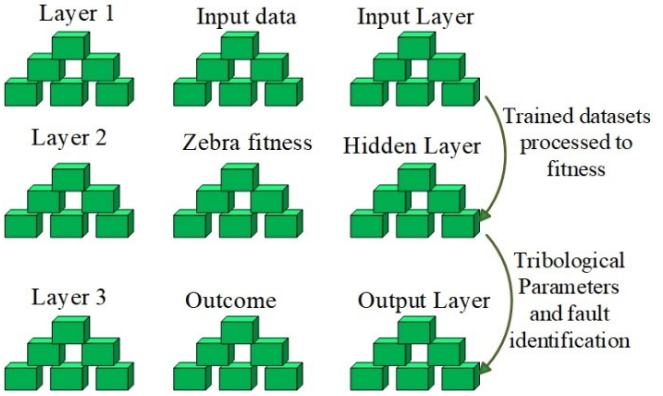

Figure 3. CAPTION.

the trained saved features. Then the performance parameters are calculated.

The proposed model explained in Figure 2, is used to identify faults from the visualized data. It depicts the process carried out in the designed ZbRBPM. The model analysed the tribological parameters from the input data to detect and classify the fault types in the thrust ball bearing. The performance criteria such as F-score, accuracy, time, wear, and friction were calculated. The F-score sometimes referred to as the F1 score or the F-measure, is a metric used to assess how well a machine learning model performs. The following sections have detailed the completed work process layers of the proposed model.

4.1. Layers of proposed ZbRBPM

The displayed novel ZbRBPM has been developed in the concept of zebra fitness and radial basis prediction mechanism. Zebra fitness is used because of its high fitness value in the optimization function. A high fitness value in the Zebra optimization function indicates that a particular solution effectively balances the thrust ball-bearing fault detection objective. It suggests the solution can accurately distinguish between faulty and healthy bearings based on the extracted features. A solution with a high fitness value is more likely to correct. Accurate fault prediction allows for preventive maintenance before catastrophic failure, saving costs associated with repairs and downtime. Numerous deep network models have been implemented for recognition with good validation of performance. However, they find it difficult to predict the approximation values. Whereas, radial basis is used for attaining the approximate function problems and it is easy to implement with strong forbearance. Here zebra fitness is applied to solve the problems and bring out the best prediction. The proposed model layers are described in Figure 3.

The proposed model has combined three phases to analyse the performance i.e. Input data phase, Zebra fitness phase, and outcome phase. At the input phase, the collected vibration signal data of the thrust ball bearing is entered and the noisy signals are filtered using the pre-processing steps. Further, at the Zebra fitness phase, the efficient features such as friction and wear tribological parameters are analysed and extracted. The analysed information is processed in the radial basis architecture to predict and classify the fault and given at the output phase of the designed model. In this training the data function is done on the input layer, the trained data undergoes the zebra fitness process in the hidden layer and this layer is high-powered, and tribological parameters and fault identification is performed. In the output layer performance analysis and classification is described. The working of the proposed model layers is described in the following section.

The raw data from the bearings is fed into the input layer. This layer trains normalizes, and pre-processes the input data. The hidden layer processes this data using the Zebra fitness function, which assesses the bearing's condition by analysing patterns and anomalies in the tribological parameters (friction and wear). Finally, the output layer demonstrates the hidden layer's processed information into particular fault predictions, indicating the presence and severity of any possible concerns.

4.2. Process of proposed ZbRBPM

The proposed ZbRBPM in the optimized network has been assisted in predicting the faults in the thrust ball bearing. In the same way, the tribological parameters like wear and friction calculations have been equated. The zebra fitness is utilized to support the classification process by (1). The dataset, which was obtained for this research is the Qatar University Dual-Machine Bearing Fault Benchmark dataset. (QU-DMBF) [33]. Here, the data are labelled data, during prediction if the vibration signal is predicted under the 0th class then it is the normal signal. If the vibration signal is predicted under 1st class then it is a ball fault. If the bearing vibration is predicted under the 2nd class then it is reported as inner race and if the predicted signal falls under the 3rd class it is determined as outer race.

$$W_{t+1} = B_t(W_{\max} - W_o) + B_t(W_{\max.t} - T_o) + W_t\,. \quad (1)$$

Here, W represents the wear, t represents the time, B_t represents the thrust bearing, W_{t+1} represents the time interval of wear, $W_{\max}$ denotes the wear maximum of the bearing, W_o represents the recorded optimal wear of the bearing, and T_o represents the recorded optimal time of the bearing. After the evaluation of wear, friction is evaluated similarly. The evaluation of friction in thrust ball bearings is described in (2)

$$F_{t+1} = B_t(F_{\max} - F_o) + B_t(F_{\max.t} - T_o) + F_t\,, \quad (2)$$

where F represents the friction, F_{t+1} represents the time interval of friction, $F_{\max}$ represents the maximum friction of the bearing, and F_o represents the recorded optimal friction of the bearing. Here the equations are derived from the zebra fitness function. The given equation analyses the wear and friction at each interval of the input vibration signal. These equations analysing the tribological parameters continuously update the vibration pattern of the given input signals to the faults. The following section defines the fault detection process.

4.3. Fault identification

Detecting the fault identification is a necessity to avert damage to the machine elements. Here, the zebra fitness accomplished the recognition faults in the detecting process. The accuracy level depends on the fitness and the trained features. The fault detecting and identification process is described below. The identification is executed in (3)

$$\eta = \text{if}\left(T\left(P_{\text{pb}}\right) = P_{\text{nb}}\right). \tag{3}$$

Here, η denotes the zebra fitness, T denotes the parameter testing, P denotes the performance, pb denotes the present bearing, and nb denotes the normal bearing. Hence the identification is performed.

Algorithm 1 shows the full explanation of the proposed model in step by step. The MATLAB system has been functioning in a step-by-step format. The output has been established.

The consecutive step for the functioning procedure of the proposed model is enumerated in the format of a flow chart is shown in Figure 4. Numerous mathematical operators are displayed in the Algorithm 1.

5. RESULT AND DISCUSSION

The MATLAB system is performed in Windows 10 and is used to validate the proposed ZbRBPM. Thrust ball bearings are utilized in cars. Thrust ball bearings assist the axial thrust of vertical and horizontal shafts. It functions to stop the shaft moving in the axial direction and transmits thrust loads practiced on the shaft. Consequently, the needed specification for the performance of the ZbRBPM is described in Table 1.

Start	
{	
	Dataset initialization
	//Initiating the observing element
	$\eta = B(W, F)$
	//Wear and friction tribological properties have been validated
	Tuning parameter
	{
	int $W_{\text{o}}, W_{\text{t}}, B_{\text{t}}, T_{\text{o}}, W_{\text{max}}$
	//Initializing the wear tuning
	Tuning $(W + 1)$
	//The thrust ball bearing wear is tuned by (1)
	int $F_{\text{o}}, F_{\text{t}}, F_{\text{max}}$
	//Initializing the friction tuning
	Tuning $(F + 1)$
	//The thrust ball bearing friction is tuned by (2)
	}
	Detecting fault
	{
	int $T, P_{\text{pb}}, P_{\text{nb}}$
	//Initializing the detection variables
	$\eta = (W_{\text{o}} + F_{\text{o}}) \cdot \beta + (P_{\text{pb}} \times P_{\text{nb}})/T$
	β -> fault prediction variable of the radial basis
	//The fault is predicted and classified
	}
}	
Stop	

Algorithm 1. ZbRBPM

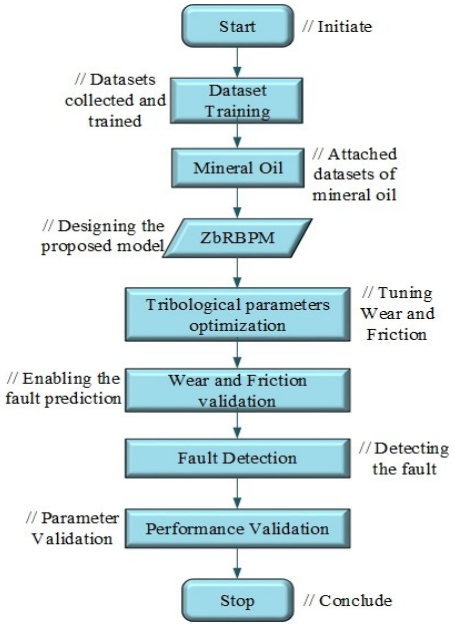

Figure 4. Flow diagram for the proposed model ZbRBPM.

Table 1. Execution parameters.

Metrics	Specification
Operating System	Windows 10
Version	3.7.14
Program	MATLAB
Dataset	Bearing image
Optimization	Zebra
Network	Radial system

5.1. Case study

This research work is made to understand the procedure of the proposed model ZbRBPM. The thrust ball-bearing datasets are taken from QU-DMBF [33]. The data is downloaded from the GitHub source.

The dataset consists of 660 vibration signals and it is divided into 80 % for training and 20 % for testing. i.e., 528 for training and 132 for testing, the description given in Figure 2. It has both the normal and faulty thrust ball bearing conditions. The faulty conditions include ball fault, inner race fault, and outer race fault. In the training phase the model is trained using the vibration signals of both the normal and faulty bearings and the model learns the different vibration types. This allows the model to distinguish between normal and faulty bearings in the operating circumstances. In the testing stage, the model is evaluated by the vibration signals data of the bearing which is not used during training the model. By exposing to both normal and faulty data during the model training, it accurately learns the behaviour of normal and faulty signal and this allows the model to identify the faults in the unseen data. It demonstrates the model's ability to generalize the new unknown data. It establishes the model's efficiency in real-world applications. The proposed methodology Zebra optimization with radial basis prediction increases the accuracy of the system under controlled circumstances. The zebra optimization enhances the model's diversity and adaptability and with the radial basis prediction it improves the model's capacity to detect and adapt to new patterns in the operations. Hence, this demonstrates better performance.

Table 2. Dataset Description.

Total Samples-660	
Normal	110
Ball Fault	165
Inner race Fault	195
Outer race Fault	190
Training Samples-528	
Normal	88
Ball Fault	132
Inner race Fault	156
Outer race Fault	152
Testing Samples-132	
Normal	22
Ball Fault	33
Inner race Fault	39
Outer race Fault	38

The fault signal in the bearing is accomplished by MATLAB is described in Figure 5.

Here, the vibration signal of the normal bearing and the fault bearing is demonstrated by the rotation of the thrust ball bearing. The normal bearings vibrations are trained to recognize the faulty vibration. The varied vibration signals are specified as the faulty vibration signals. The normalization and noise filtering process in the input layer of the presented system suppresses the false positive predictions. By analysing the tribological parameters and with the zebra fitness evaluation the model accurately distinguished the fault and normal ball bearings; also increased the reliability of the system. Some of the existing models like the Self-Driven Textured Guiding for Thrust ball bearing (SDTGT) [19], Fretting tribometer with ASTM D4170 (FTAD) [21], Voltage-Induced Damage Progression of Thrust ball bearing [23], and Self-Lubricating Polytetrafluoroethylene cages and Surface-textured raceways (SLPS) [24] are implemented in the same proposed platform for the same thrust ball bearing and compared with the proposed technique. The confusion matrix for the testing function is exposed in Figure 6.

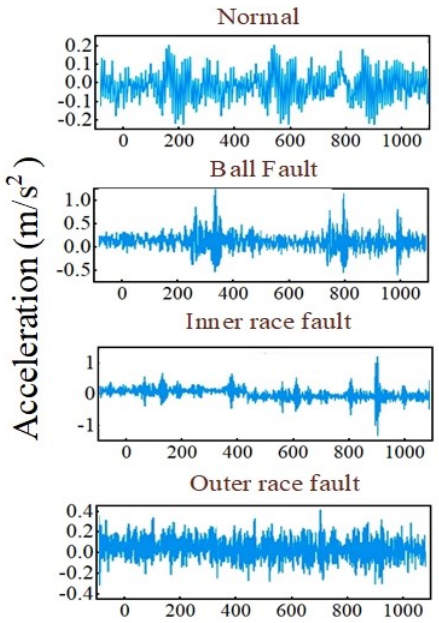

Figure 5. Normal and Faulty vibration signal of bearing.

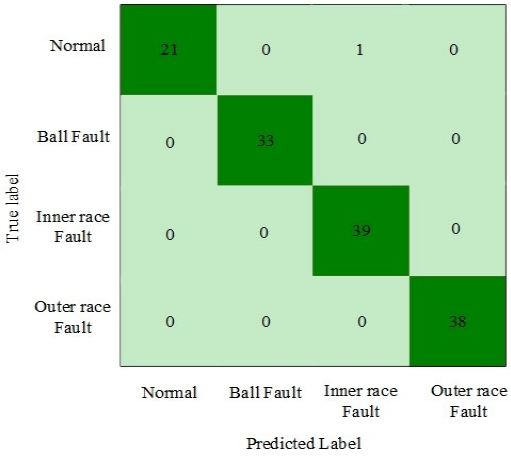

Figure 6. Confusion matrix.

5.2. Specific wear rate

The wear rate is considered to be higher for the thrust ball bearing in the bottom place of the column. The bearing in the bottom is worn more than the top. Mineral oil is almost the usual lubricant type which is utilized for thrust ball bearings. Damage wear in bearings is due to misalignment, poor installation, and improper fitting. The proposed model's specific wear rate is computed, and it is evaluated with other traditional models. The comparison is shown in Figure 7.

Here, the SDTGT has attained a specific wear rate of 1.75 mm³/(N·mm); the FTAD has attained a specific wear rate of 4.49 mm³/(N·mm), and the VIDPT has attained a specific wear rate of 2.28 mm³/(N·mm) and the SLPS has attained a specific wear rate of 3.24 mm³/(N·mm). Hence, the proposed model ZbRBPM has attained a specific wear rate of 0.35 mm³/(N·mm). Therefore, the proposed model gives the lowest wear rate compared to the prevailing models due to the zebra tuning process.

5.3. Friction torque

Friction in a thrust ball bearing is caused by improper alignment, speed, etc. Improper alignment leads to surplus force on some parts, causing wear and friction. When the rotational speed is high, the bearings' friction increased because of heat and the breakdown of lubricant. Friction is reduced by utilizing small balls and lubricating them with oil that makes the ball roll freely between the inner surface and the outer surface. The proposed model's friction torque is computed and evaluated. The comparison is shown in Figure 8.

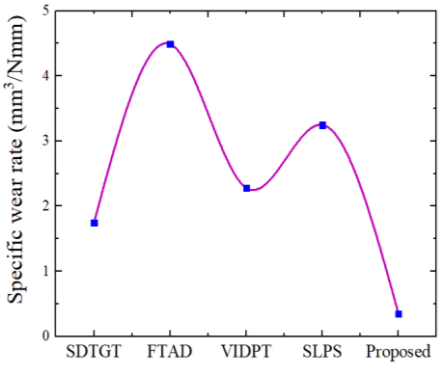

Figure 7. Specific wear rate comparison.

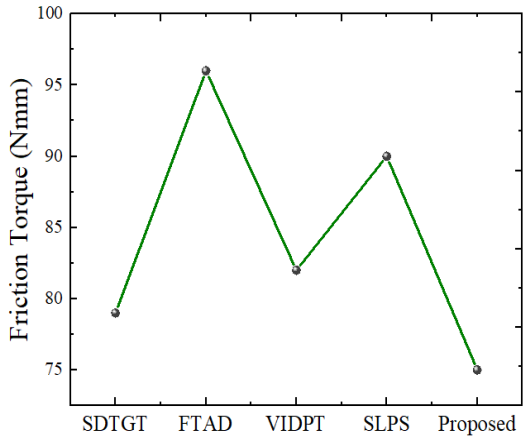

Figure 8. Friction torque comparison.

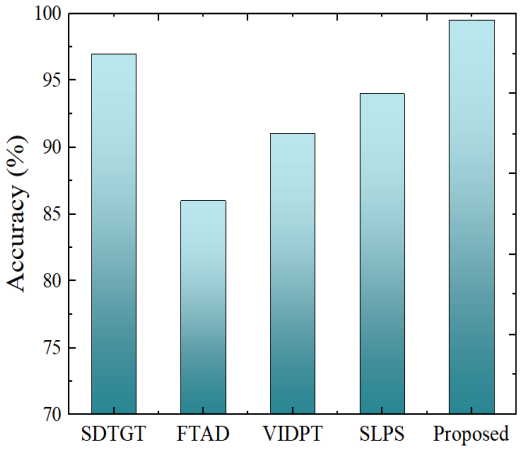

Figure 10. Accuracy comparison for fault identification.

Frictional torque is defined as the rotational force or torque required to overcome the resistance to rotation caused by the friction between the bearing components. Here, SDTGT earned a friction torque of 79 Nmm, FTAD earned a friction torque of 96 Nmm, VIDPT earned a friction torque of 82 Nmm and SLPS earned a friction torque of 90 Nmm. Hence, the proposed ZbRBPM model earned a friction torque of 75 Nmm. The proposed ZbRBPM gives the least frictional torque. In addition, energy consumption is evaluated it refers to the amount of energy required to overcome frictional resistance within the bearing during operation. It is compared with the existing techniques and displayed in Figure 9.

Excessive Frictional torque leads to energy consumption. The energy consumed by the existing techniques such as SDTGT, FTAD, VIDPT, and SLPS is 80 J, 120 J, 94 J, and 101 J respectively. The proposed ZbRBPM model consumed energy of 79 J which is low compared to the existing and hence demonstrates better performance.

5.4. Performance validation

The proposed ZbRBPM was evaluated by using the bearing visualized data and MATLAB system. The performance criteria such as Accuracy, precision, Recall, F score, Error rate, computation time, and speed were computed for the fault identification. The calculated results were made a comparison with some of the models for identifying the development of the proposed model.

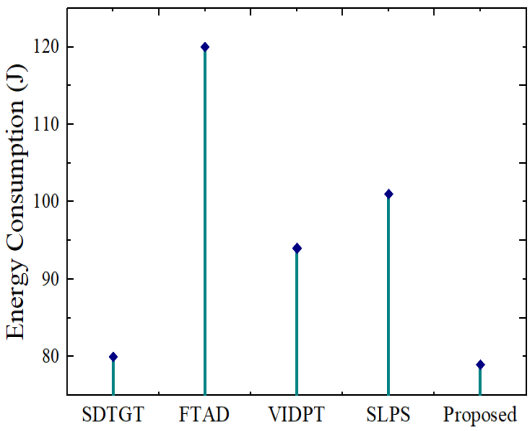

Figure 9. Energy consumption comparison.

5.5. Accuracy

The bearing's fault is evaluated by the vibration signals. The exact value estimated from the proposed model is defined as the accuracy. It is computed by the false positive, true positive, false negative, and true negative samples. Accuracy is calculated by (4)

$$Accuracy = \frac{T_N + T_P}{T_P + F_N + F_P + T_N}, \tag{4}$$

where, T_P and F_P indicate the true positive and false positive respectively, T_N and F_N indicate the true negative and false negative samples, respectively. Applying these metrics, the percentage of accuracy is calculated. The accuracy for fault identification is compared with some of the existing models and is displayed in Figure 10.

Here, the SDTGT gained an accuracy of 97 %, the FTAD gained an accuracy of 86 %, VIDPT gained an accuracy of 91 %, SLPS gained an accuracy of 94 %, and the proposed model ZbRBPM gained an accuracy of 99.5 %. Hence, the accuracy percentage the proposed ZbRBPM gains for fault identification is comparatively higher than the prevailing models. Here the accuracy value was evaluated for 132 tested signals that include all the classes. The accuracy value is accessed using the confusion matrix attained by the model. In the tested data 22 are normal signals and 110 are fault signals. The training and testing class instances are detailed in Table 2.

5.6. Precision

The estimation metrics precision calculates the positive predicting accurateness. It is evaluated by the true positive and false positive samples. The precision metrics are estimated using (5).

$$Precision = \frac{T_P}{T_P + F_P}. \tag{5}$$

The precision rate for fault identification of the proposed model is compared with some of the current models and displayed in Figure 11.

Here, the SDTGT gained a precision of 95.2 %, the FTAD gained a precision of 84.7 %, VIDPT gained a precision of 89.9 %, SLPS gained a precision of 92.6 %, and the proposed model ZbRBPM gained a precision of 99.5 %. Therefore, the Precision obtained from the proposed model is better compared to that of the prevailing models.

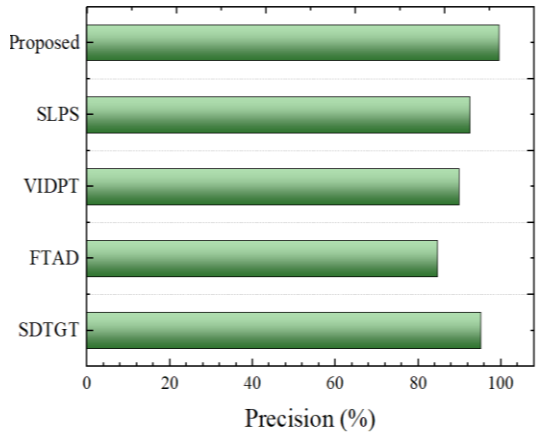

Figure 11. Precision comparison for fault identification.

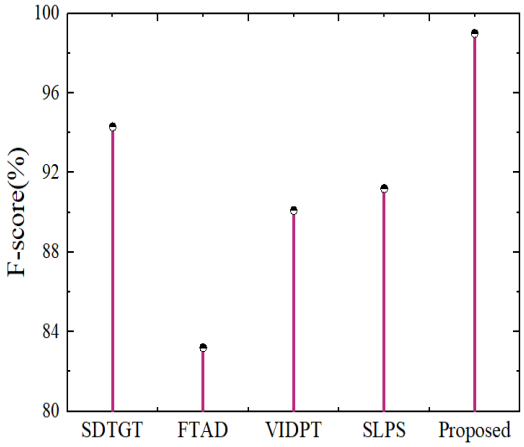

Figure 13. F-score Comparison for fault identification.

5.7. Recall

Recall is calculated by the true positive, true negative, and false negative samples. In recall metrics, the sample does not go under false positive samples. It is the calculating measure of exact identification from the regained constituents. It is evaluated using (6)

$$Recall = \frac{T_{\mathrm{P}}}{T_{\mathrm{P}} + F_{\mathrm{N}}}. \tag{6}$$

The recall rate for the fault identification of the proposed model is evaluated by applying in above (6). The comparison is displayed in Figure 12.

Here, the SDTGT obtained a Recall of 96.7 %, the FTAD obtained a Recall of 85.2 %, VIDPT obtained a Recall of 90.1 % and SLPS obtained a Recall of 92.9 %. The Recall obtained for the proposed ZbRBPM is 99.4 %. Hence, the Recall of the proposed model is high and shows a good performance.

5.8. F-Score

F score is an important metric as it combines precision and recall in an isolated value. It balances precision and recall. It is formulated by multiplying both metrics by making the sum of both metrics. The F score is evaluated by using (7)

$$Fscore = 2 \cdot \frac{R_e \cdot P_r}{R_e + P_r}. \tag{7}$$

Here, R_e represents the recall and P_r represents the precision value, and it is compared with the existing techniques and demonstrated in Figure 13.

The existing SDTGT attained 94.3 %, FTAD attained 83.2 %, VIDPT attained 90.1 % and SLPS attained 91.2 %. The F-Score for the fault identification of the proposed ZbRBPM model is 99 %. Hence, the F-score obtained from the proposed model is high and shows better performance.

5.9. Computation time

Computation time in predicting faults refers to the time duration it takes for the entire process to identify the fault in thrust ball bearing. The computation time is measured in seconds. The proposed method attained computational time is compared with the existing techniques and displayed in Figure 14.

The existing techniques attained a computation time SDTGT, FTAD, VIDPT, and SLPS of 345s, 324s, 367s, and 308s respectively. The proposed ZbRBPM model attained a computation time of 294 s, which is comparatively lower than the existing techniques and hence shows better performance.

5.10. Error rate

The error rate, referred to as the misclassification rate, represents the proportion of misclassified instances relative to the total number of instances. It is calculated by (8)

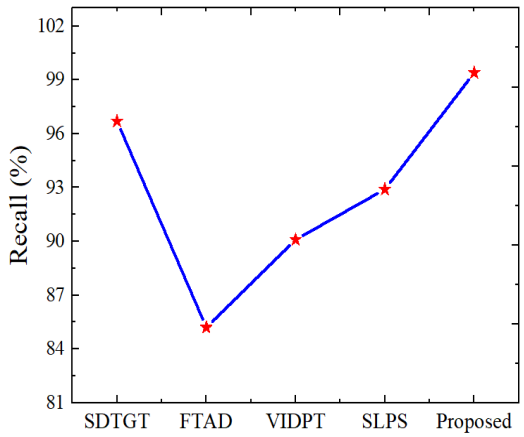

Figure 12. Recall Comparison for fault identification.

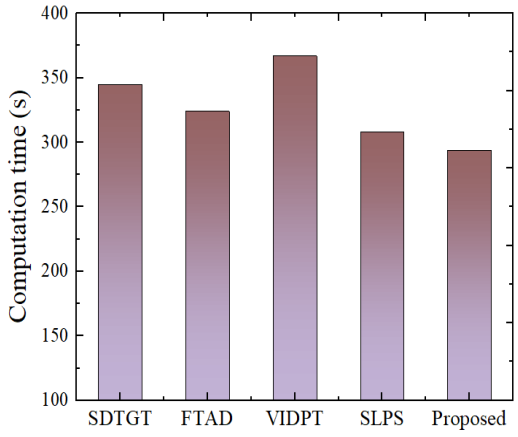

Figure 14. Computation time Comparison for fault identification.

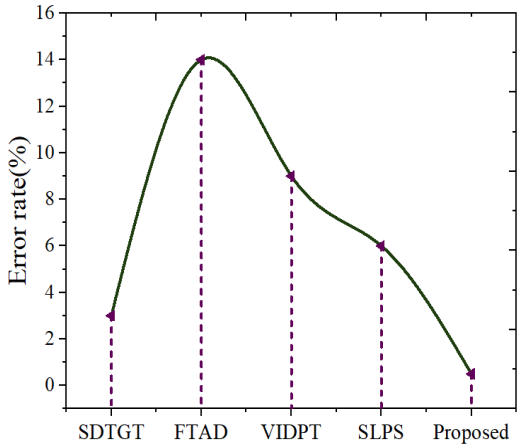

Figure 15. Error rate Comparison for fault identification.

$$ErrorRate = \frac{F_N}{F_N + T_P}. \quad (8)$$

A decrease in the error rate signifies improved performance and effectiveness in fault identification. The error rate comparison for the proposed model is shown in Figure 15.

The error rate obtained by the existing techniques is SDTGT at 3 %, FTAD is 14 %, VIDPT is 9 % and SLPS is 6 %. The proposed ZbRBPM model obtained an error rate of 0.5 %. Therefore, the error rate obtained is very low, and it demonstrates better performance of the proposed model.

5.11. Speed

Here, the prediction speed is measured in terms of Revolutions Per Minute (RPM). If the signal data is too complex, then the prediction approaches might require more time for the prediction process. Hence, to determine the prediction speed of the designed prediction mechanism, the speed parameter is taken into consideration. Validation with the existing techniques is displayed in Figure 16.

The existing techniques SDTGT, FTAD, VIDPT, and SLPS attained a speed rate of 1390 RPM, 1240 RPM, 1030 RPM, and 1450 RPM, and the proposed ZbRBPM model attained a speed rate of 1500 RPM which shows better performance by increasing the speed rate

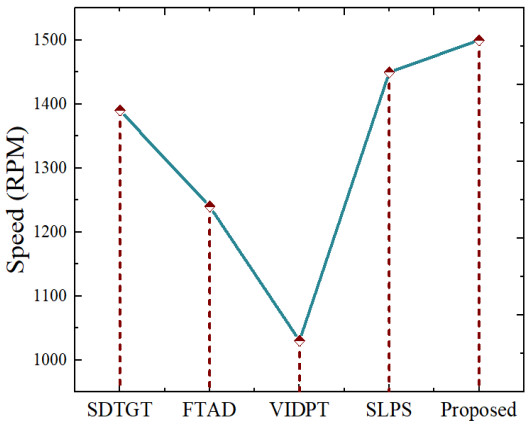

Figure 16. Speed Comparison for fault identification.

Table 3. Performance of ZbRBPM.

Metrics	Fault Identification
Accuracy	99.5 %
Precision	99 %
Recall	99.4 %
F-score	99 %
Error rate	0.5 %
Computation time	294s
Speed	1500 RPM
Specific Wear rate	0.35 mm³/Nm
Friction Torque	75Nmm

6. DISCUSSION

Usually, the deep network is utilized for prediction. But, if the data is more complex, then the prediction is not accurate. To overcome these issues, the radial basis network is enhanced with zebra optimization, which yields the optimized prediction outcome. Here, the tribological parameter wear friction is optimized by fixing the desired wear and friction rate in the zebra memory layer. While running the optimization, the algorithm is continuously iterated still a suitable solution is found.

In this present article, it is not tested in real-time scenarios, so the false positives in the true nature are not recorded. Here, the labelled database was utilized for the performance validation. In addition, the restriction of detecting faults in real time is the drawback of this study. In the future, testing the proposed model for the real-time data in a real environment will give the reliability of the system. The accomplishment of the proposed ZbRBPM is described in Table 3.

The entire performance of the proposed ZbRBPM is displayed. In this model, the zebra gives the best result for the fault identification.

To handle abnormalities, the zebra-based radial prediction mechanism is employed. This method efficiently distinguishes between normal and fault bearing from vibration signals. The Zebra optimization technique allows the model to explore several solutions and fluctuate with the environment. By fostering diversity and adaptability in the learning process, it enables the optimal function to identify the behaviour of both normal and fault-bearing data by capturing a wide range of patterns. Furthermore, based on the learned patterns the radial basis functions predict the fault, reduce the false positives, and acquire the ability to distinguish the fault by filtering the noise. This improves equipment reliability in the problem detection model, which ultimately maximizes operational efficiency overall.

7. CONCLUSION

This research paper displays the framework for thrust ball-bearing fault identification from visualized data using the optimized deep network.

To avoid failure, it is better to recognize the tribological behaviour in the bearing. MO lubrication is added to minimize wear and friction.

Zebra fitness is used to predict the fault because it has a high optimization function that gives the best prediction.

At last, the performance is validated and compared with some of the existing models. The proposed model ZbRBPM gives the

best Accuracy of 99.5 %, Precision rate of 99 %, Recall rate of 99.4 %, F-score of 99 %, Error rate of 0.5 %, and computation time is 294s.

The wear and friction obtained by the proposed model are low. The specific wear rate of the bearing is 0.35mm^3/Nm and the friction torque is 75Nmm.

The ZbRBPM proposed model accuracy is improved by 1 %. Hence, this proposed model is the most suitable for bearing fault identification.

The hybrid of zebra fitness improved the accuracy of the fault prediction. Also, the MO addition can optimize the performance of the thrust ball bearing.

By identifying potential bearing failures before catastrophic events, industries can schedule maintenance proactively, minimizing unplanned downtime. This ensures machinery remains operational for longer periods, leading to higher production output beneficial for stakeholders.

The background noise from surrounding machinery or electrical sources can mask the subtle changes in vibration signatures associated with bearing faults. Therefore the model necessitates proper filtering techniques to isolate the clear bearing-specific signal. Also, the different types of bearing faults can sometimes manifest in similar vibration patterns, which creates a complex prediction process.

The future work is to demonstrate the hybrid technique to forecast the bearing fault in real-time scenarios.

REFERENCES

[1] G. Wang, Y. Zhang, G. Liao, X. Zhang, Z. Hu, W. Wang, Experimental study on the interface topography evolution and vibration monitoring in thrust ball bearings induced by particulate contamination, J. Adv. Mech. Des. Syst. Manuf. 17(2) (2023), pp. 1-11.
DOI: 10.1299/jamdsm.2023jamdsm0029

[2] P. Khaire, V. Phalle, A smart fault identification system for ball bearing using simulation-driven vibration analysis, Arch. Mech. Eng. (2023), pp. 247-270.
DOI: 10.24425/ame.2023.145583

[3] J. J. Jayakanth, M. Chandrasekaran, R. Pugazhenthi, Impulse excitation analysis of material defects in ball bearing, Mater. Today: Proc. 39 (2021) pp. 717-724.
DOI: 10.1016/j.matpr.2020.09.305

[4] B. L. Jian, X. Y. Su, H. T. Yau, Bearing fault diagnosis based on chaotic dynamic errors in key components, IEEE Access. 9 (2021) pp. 53509-53517.
DOI: 10.1109/ACCESS.2021.3069566

[5] Z. Xie, W. Zhu, Theoretical and experimental exploration on the micro asperity contact load ratios and lubrication regimes transition for water-lubricated stern tube bearing, Tribol. Int. 164 (2021) pp. 107105.
DOI: 10.1016/j.triboint.2021.107105

[6] G. Wang, W. Wang, Y. Zhang, X. Zhang, Z. Hu, K. Liu, D. Wei, Study on micro-plastic behavior and tribological characteristics of granular materials in friction process, Ind Lubr Tribol. 73(8) (2021) pp. 1098-1104.
DOI: 10.1108/ILT-04-2021-0145

[7] Z. Xie, W. Zhu, An investigation on the lubrication characteristics of floating ring bearing with consideration of multi-coupling factors, Mech. Syst. Signal Process. 162 (2022) pp. 108086.
DOI: 10.1016/j.ymssp.2021.108086

[8] R. Liu, L. Jing, X. Meng, B. Lyu, Mixed elastohydrodynamic analysis of a coupled journal-thrust bearing system in a rotary compressor under high ambient pressure, Tribol. Int. 159 (2021) pp. 106943.
DOI: 10.1016/j.triboint.2021.106943

[9] F. Meng, J. Gong, S. Yang, L. Huang, H. Zhao, X. Tang, Study on tribo-dynamic behaviors of rolling bearing-rotor system based on neural network, Tribol. Int. 156 (2021), pp. 106829.
DOI: 10.1016/j.triboint.2020.106829

[10] Q. Qin, X. F. Wang, R. Hu, X. Cheng, Numerical investigation on single dent in EHL point contacts, Ind. Lubr. Tribol. 73(3) (2021), pp. 485-492.
DOI: 10.1108/ILT-06-2020-0215

[11] A. Hase, Early detection and identification of fatigue damage in thrust ball bearings by an acoustic emission technique, Lubricants. 8(3) (2020), pp. 37.
DOI: 10.3390/lubricants8030037

[12] A. Harder, A. Zaiat, F. M. Becker-Dombrowsky, S. Puchtler, E. Kirchner, Investigation of the voltage-induced damage progression on the raceway surfaces of thrust ball bearings, Machines. 10(10) (2022), pp. 832.
DOI: 10.3390/machines10100832

[13] V. Suthar, V. Vakharia, V. K. Patel, M. Shah, Detection of compound faults in ball bearings using multiscale-SinGAN, heat transfer search optimization, and extreme learning machine, Machines. 11(1) (2022), pp. 29.
DOI: 10.3390/machines11010029

[14] J. J. Saucedo-Dorantes, I. Zamudio-Ramirez, J. Cureno-Osornio, R. A. Osornio-Rios, J. A. Antonino-Daviu, Condition monitoring method for the detection of fault graduality in outer race bearing based on vibration-current fusion, statistical features and neural network, Applied Sciences. 11(17) (2021), pp. 8033.
DOI: 10.3390/app11178033

[15] L. Cheng, J. Lu, S. Li, R. Ding, K. Xu, X. Li, Fusion method and application of several source vibration fault signal spatio-temporal multi-correlation, Appl Sci. 11(10) (2021), pp. 4318.
DOI: 10.3390/app11104318

[16] K. Kecik, A. Smagala, K. Lyubitska, Ball Bearing Fault Diagnosis Using Recurrence Analysis, Materials, 15(17) (2022), pp. 5940.
DOI: 10.3390/ma15175940

[17] P. Ljubojević, R. Mitrović, T. Lazović, Contact Stress and Deformations in Eccentrically Loaded Thrust Ball Bearing, 10th Int. Scientific Conf. IRMES 2022 Machine design in the context of Industry 4.0–Intelligent products, Belgrade, Serbia, 26 May 2022, pp. 156-161. Online [Accessed 5 September 2024]
https://machinery.mas.bg.ac.rs/handle/123456789/6803

[18] D. Wu, X. C. Zhang, Y. F. Li, J. Wang, E. H. Han, Characterization of machined surface quality and near-surface microstructure of a high speed thrust angular contact ball bearing, J Mater Sci Technol. 86 (2021), pp. 219-226.
DOI: 10.1016/j.jmst.2020.12.074

[19] C. Wu, K. Yang, J. Ni, S. Lu, L. Yao, X. Li, Investigations for vibration and friction torque behaviors of thrust ball bearing with self-driven textured guiding surface, Friction 11(6) (2023), pp. 894-910.
DOI: 10.1007/s40544-022-0627-4

[20] V. Bhardwaj, R. K. Pandey, V. K. Agarwal, Experimental exploration for the performance improvement of a thrust ball bearing using circumferential micro-grooved races, Surf Topogr. Metrol Prop. 9(3) (2021), pp. 035017.
DOI: 10.1088/2051-672X/ac1917

[21] C. Lu-Minh, P. Njiwa, K. Leclerc, Y. M. Chen, J. Delgado, P. F. Cardey, Effectiveness of greases to prevent fretting wear of thrust ball bearings according to ASTM D4170 standard, Results Eng. 14 (2022), pp. 100468.
DOI: 10.1016/j.rineng.2022.100468

[22] W. Shan, Y. Chen, J. Huang, X. Wang, Z. Han, K. Wu, A multiphase flow study for lubrication characteristics on the internal flow pattern of ball bearing, Results Eng. 20 (2023), pp. 101429.
DOI: 10.1016/j.rineng.2023.101429

[23] S. Sun, R. Long, Z. Jin, Y. Zhang, Z. Ju, X. Du, Research on the Friction and Wear Properties of Dents Textured Rolling Element Bearings under Dry Wear, Coatings. 12(5) (2022), pp. 684.
DOI: 10.3390/coatings12050684

[24] R. Long, Z. Pan, Z. Jin, Y. Zhang, S. Sun, Y. Wang, M. Li, Tribological behavior of grooves textured thrust cylindrical roller bearings under dry wear, Adv Mech Eng. 13(12) (2021), pp. 16878140211067284.
DOI: 10.1177/16878140211067284

[25] J. Yun, B. Liu, Cobalt-removed PDC as the diamond thrust bearing friction pair material: tribological behavior in water-based drilling fluids, Tribol. Int. 189 (2023), pp. 109004.
DOI: 10.1016/j.triboint.2023.109004

[26] P. Xue, C. Chen, X. Fan, D. Diao, Current-carrying friction in carbon coated ball bearing, Friction. (2023), pp. 1-13.
DOI: 10.1007/s40544-022-0704-8

[27] J. Viola, Y. Chen, J. Wang, FaultFace: Deep convolutional generative adversarial network (DCGAN) based ball-bearing failure detection method, Information Sciences, 542 (2021), pp. 195-211.
DOI: 10.1016/j.ins.2020.06.060

[28] M. Motahari-Nezhad, S. M. Jafari, Bearing remaining useful life prediction under starved lubricating condition using time domain acoustic emission signal processing, Expert Syst. Appli. 168 (2021), pp. 114391.
DOI: 10.1016/j.eswa.2020.114391

[29] T. R. Mahesh, S. Chandrasekaran, V. Ashwin Ram, V. Vinoth Kumar, V. Vivek, S. Guluwadi, Data-driven intelligent condition adaptation of feature extraction for bearing fault detection using deep responsible active learning, IEEE Access, (2024).
DOI: 10.1109/ACCESS.2024.3380438

[30] M. T. Pham, J. M. Kim, C. H. Kim, Rolling bearing fault diagnosis based on improved GAN and 2-D representation of acoustic emission signals, IEEE Access. 10 (2022), pp. 78056-78069.
DOI: 10.1109/ACCESS.2022.3193244

[31] H. Lu, V. P. Nemani, V. Barzegar, C. Allen, C. Hu, S. Laflamme, S. Sarkar, A. T. Zimmerman, A physics-informed feature weighting method for bearing fault diagnostics, Mecha. Syst. Signal Process. 191 (2023), pp. 110171.
DOI: 10.1016/j.ymssp.2023.110171

[32] X. Fu, J. Tao, C. Qin, Q. Wei, C. Liu, A roller state-based fault diagnosis method for tunnel boring machine main bearing using two-stream CNN with multichannel detrending inputs, IEEE Trans Instrum Meas. 71 (2022), pp. 1-12.
DOI: 10.1109/TIM.2022.3212115

[33] A. Alhams, A. Abdelhadi, Y. Badri, S. Sassi, J. Renno, Enhanced Bearing Fault Diagnosis Through Trees Ensemble Method and Feature Importance Analysis, J Vib Eng Technol. (2024), pp. 1-17.
DOI: 10.1007/s42417-024-01405-0